NANO LETTERS

pubs.acs.org/NanoLett Letter

Ligand Exchange at a Covalent Surface Enables Balanced Stoichiometry in III–V Colloidal Quantum Dots

Min-Jae Choi,[§] Laxmi Kishore Sagar,[§] Bin Sun,[§] Margherita Biondi, Seungjin Lee, Amin Morteza Najjariyan, Larissa Levina, F. Pelayo García de Arquer, and Edward H. Sargent*

Cite This: https://doi.org/10.1021/acs.nanolett.1c01286 Read Online

ACCESS | Metrics & More | Article Recommendations | Supporting Information

ABSTRACT: III–V colloidal quantum dots (CQDs) are promising semiconducting materials for optoelectronic applications; however, their strong covalent character requires a distinct approach to surface management compared with widely investigated II–VI and IV–VI CQDs–dots, which by contrast are characterized by an ionic nature. Here we show stoichiometric reconstruction in InAs CQDs by ligand exchange. In particular, we find that indium–carboxylate ligands, which passivate as-synthesized InAs CQDs and are responsible for In-rich surfaces, can be replaced by anionic ligands such as thiols. This enables the production of inks consisting of balanced-stoichiometry CQDs; this is distinct from what is observed in II–VI and IV–VI CQDs, in which thiols replace carboxylates. The approach enables the implementation of InAs CQD solids as the active layer in photodiode detectors that exhibit an external quantum efficiency of 36% at 930 nm and a photoresponse time of 65 ns, which is 4 times shorter than that of reference PbS CQD devices.

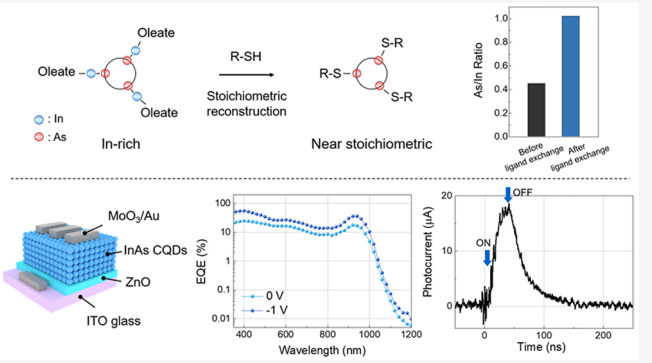

KEYWORDS: *III–V colloidal quantum dots, covalent surface, ligand exchange, stoichiometry, photodetector*

III–V colloidal quantum dots (CQDs) offer a route to field-effect transistors,[1] photodetectors,[2] short-wave infrared imaging,[3,4] and light-emitting diodes[5] that avoids regulated Pb-, Cd-, and Hg-based materials.

On the basis of previous models of II–VI and IV–VI CQDs, these are composed of a stoichiometric core with a layer of metal–ligand complexes on the surface.[6−9] This leads to CQD off-stoichiometry, which can deteriorate the optoelectronic properties by generating intragap states.[10,11] There have been recent studies of the surface chemistry of InAs CQDs[12] with the goal of improving the charge carrier mobility in devices by suppressing the surface traps observed in native InAs CQDs.[1] However, the surface and ligand chemistry of III–V CQDs is not thoroughly understood, limiting their implementation in optoelectronic applications.[13]

In this work, we found that InAs CQDs synthesized using carboxylate ligands exhibit an In-rich character, as indicated by the presence of an In–carboxylate surface shell. We then developed a ligand exchange method to control the stoichiometry of InAs CQDs. We show that X-type ligands (thiols) replace In–carboxylate ligands (Z-type), producing covalent bonding with As atoms (Scheme 1). This enables resurfacing of the In-rich CQDs and achieving balanced stoichiometry in the final CQD solid. We implemented these solids as the active layer in photodiode photodetectors, which demonstrated an external quantum efficiency (EQE) of 36%

Scheme 1. Example of Surface Ligand Exchange of CQDs Having (A) a Covalent Surface or (B) an Ionic Surface

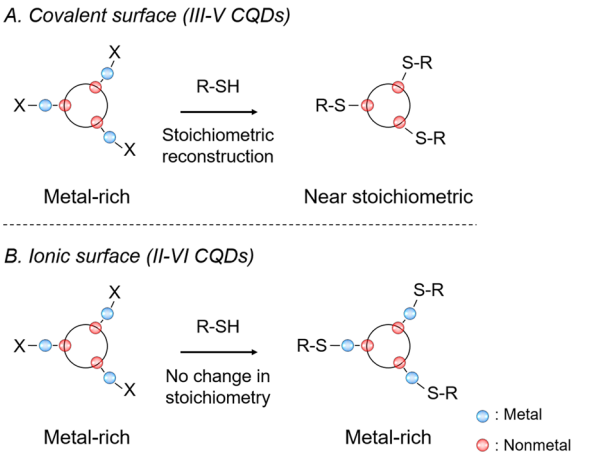

Received: March 30, 2021
Revised: July 5, 2021

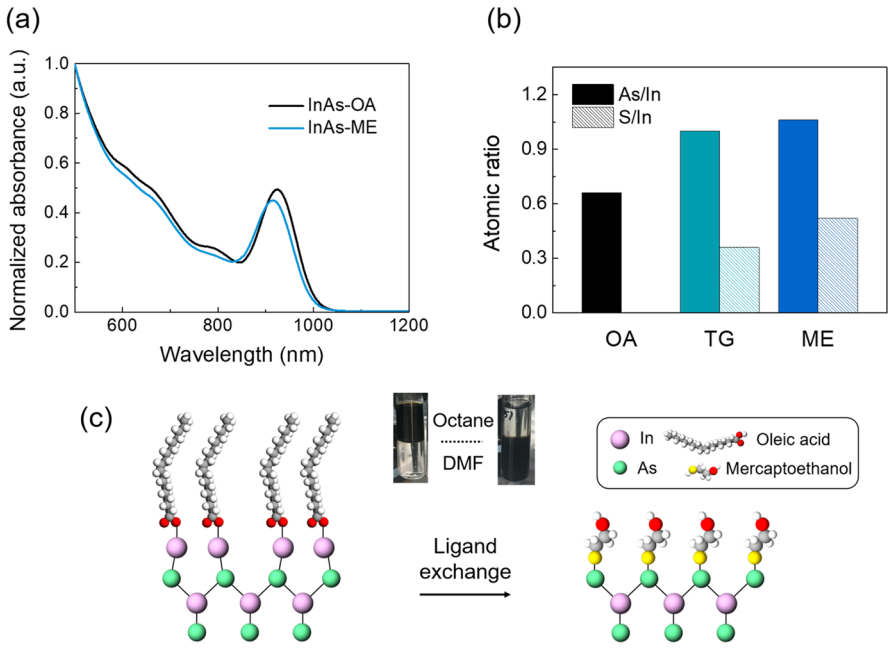

Figure 1. (a) UV−vis absorption spectrum of InAs CQDs before ligand exchange (black, OA ligands) and after ligand exchange (blue, ME ligands). (b) XPS atomic ratios of InAs CQDs before and after ligand exchange. (c) Schematic illustration of InAs CQDs before and after ligand exchange. The inset photographs show phase transfer of InAs CQDs from a nonpolar solvent (octane) to a polar solvent (DMF) after ligand exchange.

under reverse bias (−1 V) with monochromatic illumination at 940 nm. The photoresponse time of these new InAs CQD devices is 65 ns, which is 4 times shorter than that of reference PbS CQD devices.

We began by synthesizing InAs CQDs via a modification of a previous method using indium acetate, oleic acid (OA), and tris(trimethylgermyl)arsine ($(TMGe)_3As$) (see the Supporting Information). The as-synthesized CQDs were capped with OA and showed an absorption peak ($1S_{max}$) at 920 nm (Figure 1a). We found that the lower reactivity of $(TMGe)_3As$ compared with $(TMSi)_3As$[14] enables a narrower CQD size distribution compared with prior reports,[15] resulting in a 60 meV half width at half-maximum.

X-ray photoelectron spectroscopy (XPS) measurements revealed that the as-synthesized CQDs exhibit an In-rich stoichiometry (Figure 1b, As/In ≈ 0.7). We can account for this via a model in which the OA-capped InAs CQDs consist of an inorganic InAs core and an indium−oleate ligand shell (Scheme 1), resulting in a metal-rich character similar to that of OA-capped PbS CQDs.[7,16] CQD off-stoichiometry is known to lead to intragap states, which deteriorate charge transport, promote nonradiative recombination, and preclude efficient optoelectronic operation.[10,11]

We therefore sought to control the stoichiometry of the InAs CQDs. Our approach to achieve stoichiometric balance was to remove the indium−oleate shell that renders the In-rich character. We reasoned that thiol ligands could replace indium−oleate ligands and make covalent bonds with the surface As atoms, as reported in bulk InAs.[17,18] To this end, we designed solution-phase ligand exchanges based on 2-mercaptoethanol (ME) molecules. OA-capped InAs CQDs dissolved in octane were vigorously mixed with the ligand solution in *N*,*N*-dimethylformamide (DMF). The CQDs were then transferred from the octane phase to the DMF phase (Figure 1c). The InAs CQD inks retained their homogeneity after ligand exchange, as shown by absorption measurements (Figure 1a), and remained stable as colloids for hours (Figure S1). The formation of a stable colloid of CQDs in DMF implies that InAs CQDs are stabilized by electrostatic stabilization, similar to previous reports on PbS CQDs.[19,20] The slight blue shift in the wavelength of the lowest-energy absorption spectral feature ($1S_e \rightarrow 1S_h$) may be explained by the exchange of indium−oleate ligands with thiols, which results in a slight decrease in the effective size of the InAs CQDs.[21,22]

Transmission electron microscopy (TEM) revealed a reduced interdot distance following exchange (Figure S2), which indicates successful ligand exchange on the InAs CQDs. Fourier transform infrared (FT-IR) spectroscopy further confirmed the complete exchange of oleic acid (Figure S3). The S 2p XPS spectrum of ME-exchanged InAs CQDs shows the presence of sulfur, indicating that the CQD surfaces are passivated with thiol ligands (Figure S4). In addition, the ME-exchanged CQDs exhibit stoichiometry between In and As (Figure 1b). We found that other thiol molecules [1-thioglycerol (TG)] show similar results. To study any change of stoichiometry before and after ligand exchange, we performed energy-dispersive X-ray (EDX) analysis of InAs CQD solids (Figure S5 and Table S1). This revealed that ligand exchange produces a balanced stoichiometry between In and As, while the InAs CQD solids exhibit an In-rich stoichiometry before ligand exchange.

To further understand the interaction between the CQD surface and ligands, we analyzed the XPS spectra of other elements, including C, In, and As. The C 1s XPS spectra confirm that the ligand exchange results in complete removal of the COO^- peak at 288.8 eV, a signal of OA ligands (Figure 2a,d). This result agrees with the In 3d spectra showing the disappearance of the indium−oleate peak after ligand exchange (Figure 2b,e). Interestingly, no thiol shoulder peak is visible in the In 3d spectra, while a thiol peak is present in the As 3d spectra. Specifically, ME-exchanged CQDs exhibit an As−S

https://doi.org/10.1021/acs.nanolett.1c01286
Nano Lett. XXXX, XXX, XXX−XXX

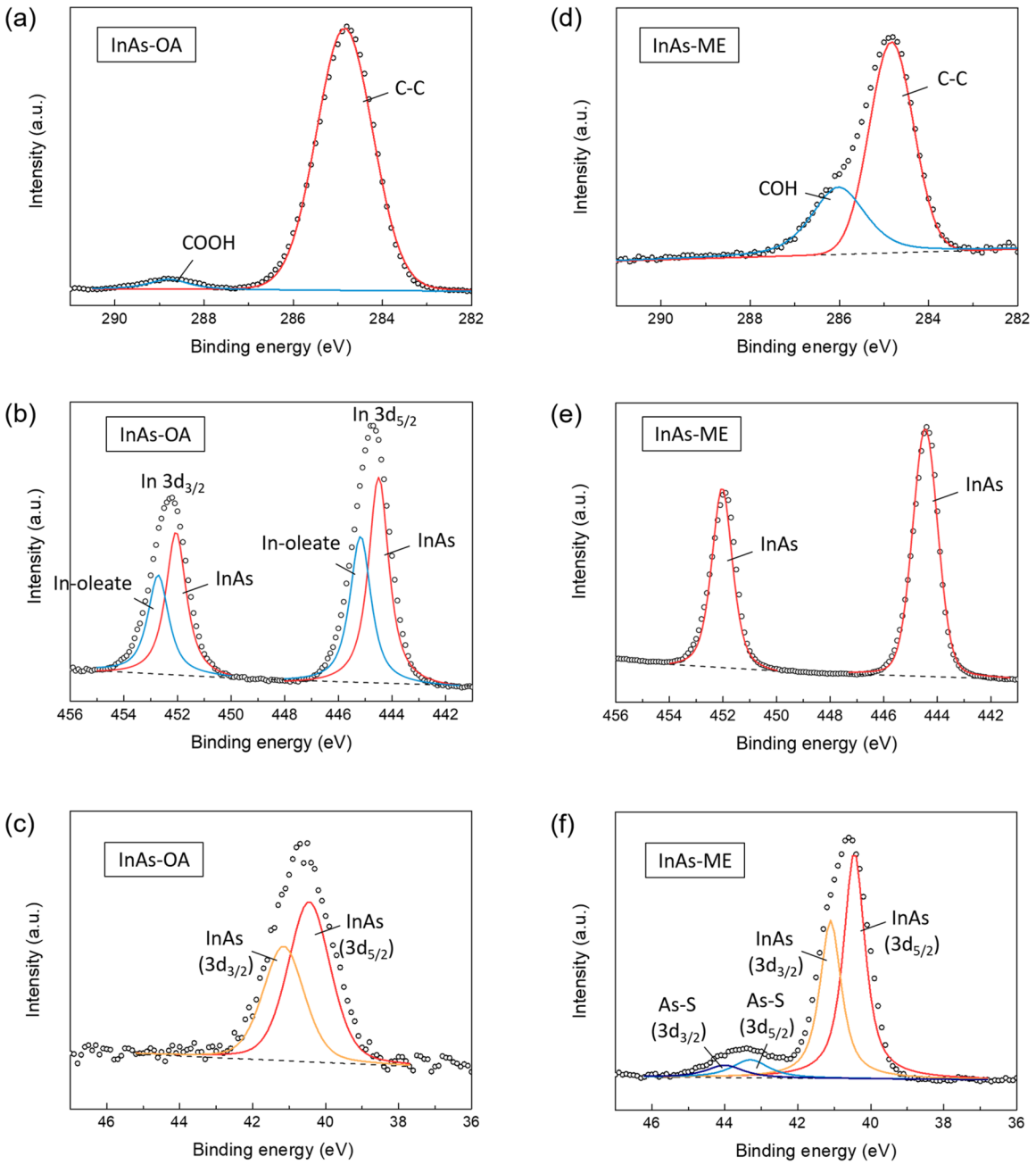

Figure 2. XPS spectra of InAs CQDs (a–c) before and (d–f) after ligand exchange: (a, d) C 1s spectra; (b, e) In 3d spectra; (c, f) As 3d spectra. Further information on these spectra is provided in Table S2.

peak at around 43.5 eV[23,24] that is not observed before ligand exchange (Figure 2c,f). The XPS data support the hypothesis discussed in Figure 1c that the initial In–oleate ligands are exchanged with thiol ligands. This can be explained by covalent bonding between As and thiol, which is consistent with the covalent nature of InAs and not observed in ionic II–VI and IV–VI CQDs (Scheme 1). In addition, a high concentration of thiol ligands during ligand exchange may promote As–S binding dominantly rather than In–S binding.[17]

To investigate the impact of the surface chemistry on the CQD defect density, we sought to measure the Stokes shift of the CQDs. The Stokes shift of CQDs allows a relative comparison among trap densities of CQDs with different surface ligands;[25] in contrast, photoluminescence can decrease after ligand exchange with shorter ligands,[26,27] even in cases where the ligand exchange provides lower trap densities.[28−30] We measured the absorbance and photoluminescence of InAs CQDs with different surface ligands (Figure 3a). Acetic acid (AA) ligands were also used for comparison, since these have the same length as ME but a different functional group. The as-synthesized CQDs (OA ligands) exhibit a Stokes shift of 76 meV, which decreases to 47 meV after ligand exchange with ME ligands (Figure 3b). Ligand exchange using AA leads to a Stokes shift of 65 meV, which is larger than for ME-exchanged CQDs. This suggests that surface chemistry modification with ME minimizes the CQD defect density.[25] In addition, the full width at half-maximum (fwhm) of the CQD emission spectra is preserved after ligand exchange with ME, indicating that CQD homogeneity is retained.

https://doi.org/10.1021/acs.nanolett.1c01286
Nano Lett. XXXX, XXX, XXX−XXX

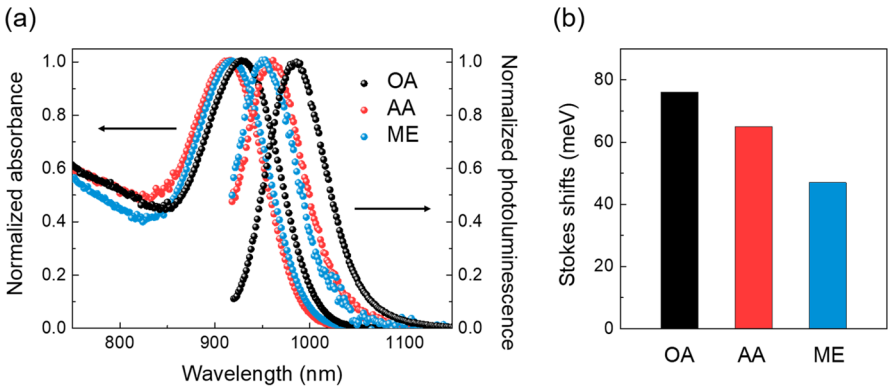

Figure 3. (a) Normalized absorbance and photoluminescence spectra of InAs CQDs with different surface ligands in solution. (b) Stokes shifts of CQDs calculated from (a). A 1 mg/mL CQD solution was used for all samples.

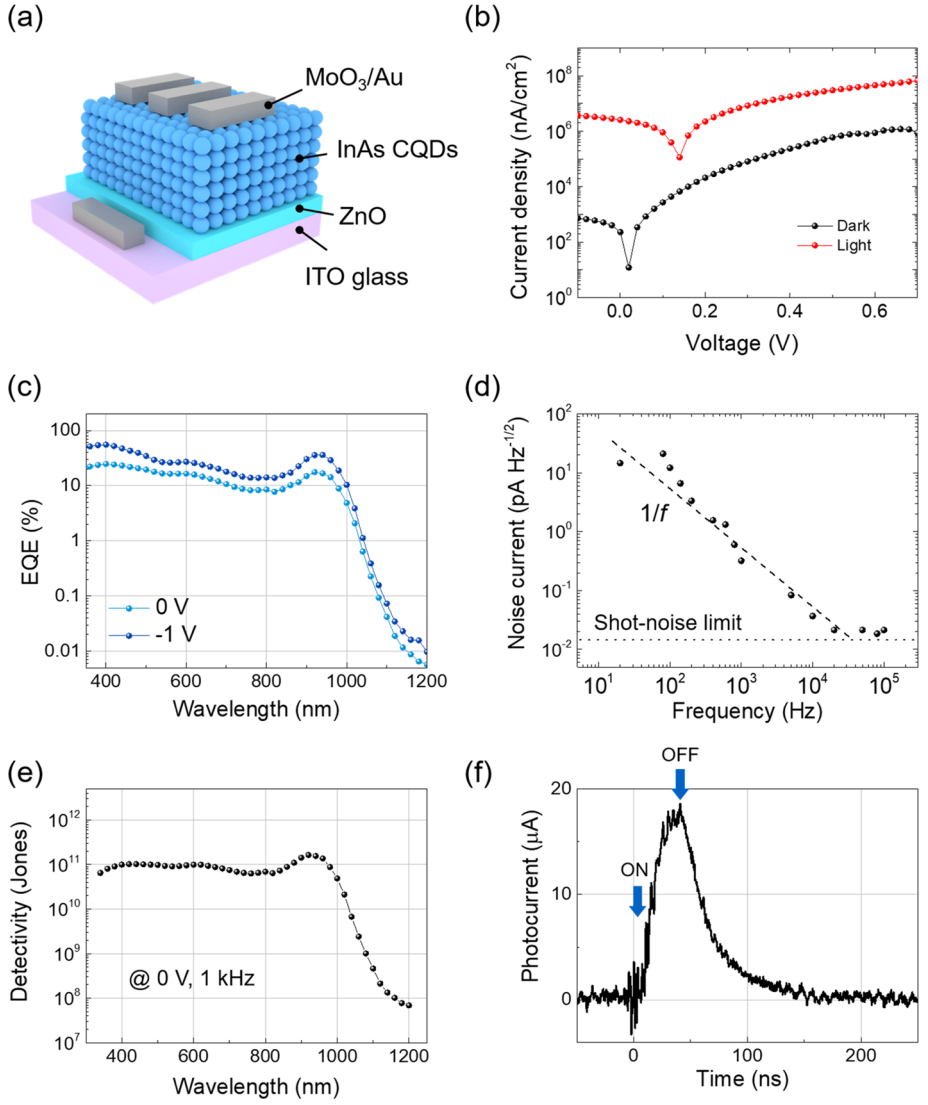

Figure 4. (a) Schematic illustration of InAs CQD photodiodes. (b) $J-V$ characteristic of the device under dark conditions and under 1 sun illumination. (c) External quantum efficiency (EQE) measurement of the device. (d) Dependence of the noise current on the frequency at 0 V. (e) Specific detectivity spectrum under the operating conditions of 0 V and 1 kHz. (f) Photoresponse dynamics at 0 V with a 39 ns pulsed laser. The inset image shows magnified photoresponse with fall time of 65 ns.

We then implemented the resulting InAs-ME CQD solids as the active layer in photodiode photodetectors. The device configuration comprises a transparent conductive indium tin oxide (ITO) bottom electrode (~160 nm); a ZnO electron transport layer (~180 nm); the photoactive layer of ME-exchanged CQDs (~100 nm); a MoO_3 hole transport layer

https://doi.org/10.1021/acs.nanolett.1c01286
Nano Lett. XXXX, XXX, XXX−XXX

(~10 nm); and a Au metal top electrode (~160 nm), as shown in Figure 4a.

The devices show rectifying behavior, with a rectification ratio [defined as $I_{dark}(1\ V)/I_{dark}(-1\ V)$] of 7050 under dark conditions (Figures 4b and S6). At 0 V, the devices exhibit an EQE of 18% at the excitonic peak. The EQE spectrum matches the absorption of the CQDs. The dependence of the EQE spectrum on the applied bias reveals that the devices are not fully depleted under short-circuit conditions, as the EQE gradually increased to 36% at −1 V reverse bias (Figure 4c). To our knowledge, this is the first report of photodiodes based on InAs CQDs.

To study the impact of the InAs CQD surface chemistry on the device characteristics, we prepared InAs CQD photodiodes using AA as a surface ligand. The devices exhibited a rectification ratio of 7 under dark conditions and an EQE of <1% (Figures S7 and S8) when the same device structure as shown in Figure 4a was employed. XPS measurements showed that InAs-AA CQD solids have a stoichiometry of ~0.8 (Table S3). The balanced stoichiometry of InAs-ME CQDs compared with InAs-AA CQDs results in a reduced defect density, as shown in Figure 3. This also leads to higher EQE values at all wavelengths and lower leakage current under dark conditions.

We evaluated the sensitivity of the InAs CQD photodiodes and characterized their noise under various operating frequencies (Figure 4d). Under short-circuit conditions, the noise current gradually decreases with increasing operation frequency and flattens at around 10 kHz to a value of 2 times the shot-noise limit. This behavior is typical of flicker noise, as previously reported in CQD photodetectors.[31,32]

The measured specific detectivity reaches 1.6×10^{11} Jones at the excitonic peak (1 kHz) (Figure 4e). We further characterized the photoresponse of the InAs CQD photodetectors with a 39 ns width pulsed laser (repetition frequency of 1 MHz). We observed stable photoresponse and a fall time of 65 ns for a device with an area of 0.8 mm^2 (Figure 4f).

To evaluate the performance of InAs CQD photodetectors, we compare these results with best photodiodes based on PbS CQDs operating at similar wavelengths (~950 nm).[33] The InAs devices show an ~4 times faster temporal response following transient photoexcitation, with a fall time of ~65 ns, compared with 250 ns for PbS CQD devices (Figure S9). In general, improved response times in photosensors can enable both higher-frame-rate light sensors and also LIDAR for time-of-flight applications. The results suggest the potential of InAs CQDs as a heavy-metal-free active material in optoelectronic devices and indicate routes for further progress in InAs colloid management and devices.

In sum, here we have offered new insights into the surface interactions of III−V CQDs and their impact on efficient optoelectronic operation. Our findings reveal that covalent bonding of InAs CQDs with ligands enables a different surface configuration that is not shown in II−VI and IV−VI CQDs. On the basis of this knowledge, we have demonstrated stoichiometry-controlled InAs CQDs through ligand exchange. This translates into photodiode detectors exhibiting a specific detectivity of 1.6×10^{11} Jones and a photoresponse time of 65 ns. This work opens the door to the realization of high-performance optoelectronic devices based on III−V CQDs.

■ ASSOCIATED CONTENT

Supporting Information

The Supporting Information is available free of charge at https://pubs.acs.org/doi/10.1021/acs.nanolett.1c01286.

Experimental details of the synthesis of CQDs, ligand exchange, fabrication of CQD photodiodes, and characterizations (*J*−*V*, EQE, PL, absorption measurement, XPS, TEM, transient photocurrent) (PDF)

■ AUTHOR INFORMATION

Corresponding Author

Edward H. Sargent − *Department of Electrical and Computer Engineering, University of Toronto, Toronto, Ontario M5S 3G4, Canada;* orcid.org/0000-0003-0396-6495; Email: ted.sargent@utoronto.ca

Authors

Min-Jae Choi − *Department of Electrical and Computer Engineering, University of Toronto, Toronto, Ontario M5S 3G4, Canada; Department of Chemical and Biochemical Engineering, Dongguk University, Seoul 04620, Republic of Korea;* orcid.org/0000-0002-6699-1703

Laxmi Kishore Sagar − *Department of Electrical and Computer Engineering, University of Toronto, Toronto, Ontario M5S 3G4, Canada;* orcid.org/0000-0002-7656-7308

Bin Sun − *Department of Electrical and Computer Engineering, University of Toronto, Toronto, Ontario M5S 3G4, Canada;* orcid.org/0000-0002-8233-0999

Margherita Biondi − *Department of Electrical and Computer Engineering, University of Toronto, Toronto, Ontario M5S 3G4, Canada*

Seungjin Lee − *Department of Electrical and Computer Engineering, University of Toronto, Toronto, Ontario M5S 3G4, Canada;* orcid.org/0000-0002-6318-0702

Amin Morteza Najjariyan − *Department of Electrical and Computer Engineering, University of Toronto, Toronto, Ontario M5S 3G4, Canada*

Larissa Levina − *Department of Electrical and Computer Engineering, University of Toronto, Toronto, Ontario M5S 3G4, Canada*

F. Pelayo García de Arquer − *Department of Electrical and Computer Engineering, University of Toronto, Toronto, Ontario M5S 3G4, Canada;* orcid.org/0000-0003-2422-6234

Complete contact information is available at: https://pubs.acs.org/10.1021/acs.nanolett.1c01286

Author Contributions

[§]M.-J.C., L.K.S., and B.S. contributed equally. The manuscript was written through contributions of all authors. All of the authors approved the final version of the manuscript.

Funding

This work was supported by an NSERC Discovery Grant and Canada Research Chair and by a National Research Foundation of Korea (NRF) grant funded by the Government of Korea (MSIT) (2021R1A4A3024237).

Notes

The authors declare no competing financial interest.

■ ACKNOWLEDGMENTS

We thank D. Kopilovic, E. Palmiano, and R. Wolowiec for technical support.

■ REFERENCES

(1) Song, J. H.; Choi, H.; Pham, H. T.; Jeong, S. Energy level tuned indium arsenide colloidal quantum dot films for efficient photovoltaics. *Nat. Commun.* **2018**, *9*, 4267.
(2) Zhao, T. S.; Oh, N.; Jishkariani, D.; Zhang, M. L.; Wang, H.; Li, N.; Lee, J. D.; Zeng, C. J.; Muduli, M.; Choi, H. J.; Su, D.; Murray, C. B.; Kagan, C. R. General Synthetic Route to High-Quality Colloidal III-V Semiconductor Quantum Dots Based on Pnictogen Chlorides. *J. Am. Chem. Soc.* **2019**, *141*, 15145−15152.
(3) Franke, D.; Harris, D. K.; Chen, O.; Bruns, O. T.; Carr, J. A.; Wilson, M. W. B.; Bawendi, M. G. Continuous injection synthesis of indium arsenide quantum dots emissive in the short-wavelength infrared. *Nat. Commun.* **2016**, *7*, 12749.
(4) Ren, D. K.; Meng, X.; Rong, Z. X.; Cao, M.; Farrell, A. C.; Somasundaram, S.; Azizur-Rahman, K. M.; Williams, B. S.; Huffaker, D. L. Uncooled Photodetector at Short-Wavelength Infrared Using InAs Nanowire Photoabsorbers on InP with p-n Heterojunctions. *Nano Lett.* **2018**, *18*, 7901−7908.
(5) Won, Y. H.; Cho, O.; Kim, T.; Chung, D. Y.; Kim, T.; Chung, H.; Jang, H.; Lee, J.; Kim, D.; Jang, E. Highly efficient and stable InP/ZnSe/ZnS quantum dot light-emitting diodes. *Nature* **2019**, *575*, 634−638.
(6) Dubois, F.; Mahler, B.; Dubertret, B.; Doris, E.; Mioskowski, C. A versatile strategy for quantum dot ligand exchange. *J. Am. Chem. Soc.* **2007**, *129*, 482−483.
(7) Anderson, N. C.; Hendricks, M. P.; Choi, J. J.; Owen, J. S. Ligand Exchange and the Stoichiometry of Metal Chalcogenide Nanocrystals: Spectroscopic Observation of Facile Metal-Carboxylate Displacement and Binding. *J. Am. Chem. Soc.* **2013**, *135*, 18536−18548.
(8) Gomes, R.; Hassinen, A.; Szczygiel, A.; Zhao, Q. A.; Vantomme, A.; Martins, J. C.; Hens, Z. Binding of Phosphonic Acids to CdSe Quantum Dots: A Solution NMR Study. *J. Phys. Chem. Lett.* **2011**, *2*, 145−152.
(9) Hassinen, A.; Moreels, I.; De Nolf, K.; Smet, P. F.; Martins, J. C.; Hens, Z. Short-Chain Alcohols Strip X-Type Ligands and Quench the Luminescence of PbSe and CdSe Quantum Dots, Acetonitrile Does Not. *J. Am. Chem. Soc.* **2012**, *134*, 20705−20712.
(10) Zherebetskyy, D.; Zhang, Y. J.; Salmeron, M.; Wang, L. W. Tolerance of Intrinsic Defects in PbS Quantum Dots. *J. Phys. Chem. Lett.* **2015**, *6*, 4711−4716.
(11) Li, Y.; Hou, X. Q.; Dai, X. L.; Yao, Z. L.; Lv, L. L.; Jin, Y. Z.; Peng, X. G. Stoichiometry-Controlled InP-Based Quantum Dots: Synthesis, Photoluminescence, and Electroluminescence. *J. Am. Chem. Soc.* **2019**, *141*, 6448−6452.
(12) Leemans, J.; Dümbgen, K. C.; Minjauw, M. M.; Zhao, Q.; Vantomme, A.; Infante, I.; Detavernier, C.; Hens, Z. Acid−Base Mediated Ligand Exchange on Near-Infrared Absorbing, Indium-Based III−V Colloidal Quantum Dots. *J. Am. Chem. Soc.* **2021**, *143*, 4290−4301.
(13) Kim, Y.; Chang, J. H.; Choi, H.; Kim, Y. H.; Bae, W. K.; Jeong, S. III-V colloidal nanocrystals: control of covalent surfaces. *Chem. Sci.* **2020**, *11*, 913−922.
(14) Harris, D. K.; Bawendi, M. G. Improved Precursor Chemistry for the Synthesis of III-V Quantum Dots. *J. Am. Chem. Soc.* **2012**, *134*, 20211−20213.
(15) Tamang, S.; Lee, S.; Choi, H.; Jeong, S. Tuning Size and Size Distribution of Colloidal InAs Nanocrystals via Continuous Supply of Prenucleation Clusters on Nanocrystal Seeds. *Chem. Mater.* **2016**, *28*, 8119−8122.
(16) Choi, H.; Ko, J. H.; Kim, Y. H.; Jeong, S. Steric-Hindrance-Driven Shape Transition in PbS Quantum Dots: Understanding Size-Dependent Stability. *J. Am. Chem. Soc.* **2013**, *135*, 5278−5281.
(17) Losurdo, M.; Wu, P. C.; Kim, T. H.; Bruno, G.; Brown, A. S. Cysteamine-Based Functionalization of InAs Surfaces: Revealing the Critical Role of Oxide Interactions in Biasing Attachment. *Langmuir* **2012**, *28*, 1235−1245.
(18) Knorr, D.; Tran, N.; Williams, K.; Andzelm, J.; Henry, N.; Gaskell, K.; Lenhart, J.; Baril, N.; Jaye, C.; Fischer, D.; Tidrow, M.; Bandara, S. Bonding of cysteamine on InAs surfaces. *Appl. Surf. Sci.* **2018**, *462*, 489−501.
(19) Dirin, D. N.; Dreyfuss, S.; Bodnarchuk, M. I.; Nedelcu, G.; Papagiorgis, P.; Itskos, G.; Kovalenko, M. V. Lead Halide Perovskites and Other Metal Halide Complexes as Inorganic Capping Ligands for Colloidal Nanocrystals. *J. Am. Chem. Soc.* **2014**, *136*, 6550−6553.
(20) Aqoma, H.; Jang, S.-Y. Solid-state-ligand-exchange free quantum dot ink-based solar cells with an efficiency of 10.9%. *Energy Environ. Sci.* **2018**, *11*, 1603−1609.
(21) Tang, J.; Brzozowski, L.; Barkhouse, D. A. R.; Wang, X. H.; Debnath, R.; Wolowiec, R.; Palmiano, E.; Levina, L.; Pattantyus-Abraham, A. G.; Jamakosmanovic, D.; Sargent, E. H. Quantum Dot Photovoltaics in the Extreme Quantum Confinement Regime: The Surface-Chemical Origins of Exceptional Air- and Light-Stability. *ACS Nano* **2010**, *4*, 869−878.
(22) Choi, M. J.; Oh, J.; Yoo, J. K.; Choi, J.; Sim, D. M.; Jung, Y. S. Tailoring of the PbS/metal interface in colloidal quantum dot solar cells for improvements of performance and air stability. *Energy Environ. Sci.* **2014**, *7*, 3052−3060.
(23) Fukuda, Y.; Suzuki, Y.; Sanada, N.; Shimomura, M.; Masuda, S. $(NH_4)_2S_x$-treated InAs (001) surface studied by X-ray photoelectron spectroscopy and low-energy electron diffraction. *Phys. Rev. B: Condens. Matter Mater. Phys.* **1997**, *56*, 1084.
(24) Khdary, N. H.; Gassim, A. E. H.; Howard, A. G.; Sakthivel, T. S.; Seal, S. Synthesis and modification of mercapto-submicron scavenger for real-time extraction and preconcentration of As(III). *Anal. Methods* **2018**, *10*, 245−255.
(25) Liu, Y.; Kim, D.; Morris, O. P.; Zhitomirsky, D.; Grossman, J. C. Origins of the Stokes Shift in PbS Quantum Dots: Impact of Polydispersity, Ligands, and Defects. *ACS Nano* **2018**, *12*, 2838−2845.
(26) Zhao, C.; Bai, Z.; Liu, X.; Zhang, Y.; Zou, B.; Zhong, H. Small GSH-Capped CuInS2 Quantum Dots: MPA-Assisted Aqueous Phase Transfer and Bioimaging Applications. *ACS Appl. Mater. Interfaces* **2015**, *7*, 17623−17629.
(27) Lesiak, A.; Banski, M.; Halicka, K.; Cabaj, J.; Zak, A.; Podhorodecki, A. pH-dependent fluorescence of thiol-coated CdSe/CdS quantum dots in an aqueous phase. *Nanotechnology* **2021**, *32*, 075705.
(28) Ding, C.; Liu, F.; Zhang, Y.; Hayase, S.; Masuda, T.; Wang, R.; Zhou, Y.; Yao, Y.; Zou, Z.; Shen, Q. Passivation Strategy of Reducing Both Electron and Hole Trap States for Achieving High-Efficiency PbS Quantum-Dot Solar Cells with Power Conversion Efficiency over 12%. *ACS Energy Lett.* **2020**, *5*, 3224−3236.
(29) Niu, G.; Wang, L.; Gao, R.; Ma, B.; Dong, H.; Qiu, Y. Inorganic iodide ligands in ex situ PbS quantum dot sensitized solar cells with I^-/I_3^- electrolytes. *J. Mater. Chem.* **2012**, *22*, 16914−16919.
(30) Liu, J.; Zhang, H.; Navarro-Pardo, F.; Selopal, G. S.; Sun, S.; Wang, Z. M.; Zhao, H.; Rosei, F. Hybrid surface passivation of PbS/CdS quantum dots for efficient photoelectrochemical hydrogen generation. *Appl. Surf. Sci.* **2020**, *530*, 147252.
(31) Liu, H.; Lhuillier, E.; Guyot-Sionnest, P. 1/f noise in semiconductor and metal nanocrystal solids. *J. Appl. Phys.* **2014**, *115*, 154309.
(32) García de Arquer, F. P.; Gong, X. W.; Sabatini, R. P.; Liu, M.; Kim, G. H.; Sutherland, B. R.; Voznyy, O.; Xu, J. X.; Pang, Y. J.; Hoogland, S.; Sinton, D.; Sargent, E. Field-emission from quantum-dot-in-perovskite solids. *Nat. Commun.* **2017**, *8*, 14757.
(33) Sun, B.; Johnston, A.; Xu, C.; Wei, M.; Huang, Z.; Jiang, Z.; Zhou, H.; Gao, Y.; Dong, Y.; Ouellette, O.; Zheng, X.; Liu, J.; Choi, M.-J.; Gao, Y.; Baek, S.-W.; Laquai, F.; Bakr, O. M.; Ban, D.; Voznyy, O.; Garcia de Arquer, F. P.; Sargent, E. H. Monolayer Perovskite

https://doi.org/10.1021/acs.nanolett.1c01286
Nano Lett. XXXX, XXX, XXX−XXX

Bridges Enable Strong Quantum Dot Coupling for Efficient Solar Cells. *Joule* **2020**, *4*, 1542−1556.

https://doi.org/10.1021/acs.nanolett.1c01286
Nano Lett. XXXX, XXX, XXX−XXX